

UCRL--92705

DE87 008158

TECHNOLOGY DEVELOPMENT FOR HIGH POWER INDUCTION ACCELERATORS

D. L. Birx
L. L. Reginato

This paper was prepared for submittal to
Second N.C. Christophilos International Conference
On Pulsed Power & Its Applications
Island of Spetses, Greece
August 5-9, 1985

June 11, 1985

The logo of Lawrence Livermore National Laboratory is a large, stylized 'V' shape. The top horizontal bar is white, the middle bar is grey, and the bottom bar is black. The text 'Lawrence Livermore National Laboratory' is written in a sans-serif font, rotated 45 degrees counter-clockwise, and positioned within the right-hand side of the 'V' shape.

Lawrence
Livermore
National
Laboratory

This is a preprint of a paper intended for publication in a journal or proceedings. Since changes may be made before publication, this preprint is made available with the understanding that it will not be cited or reproduced without the permission of the author.

DISTRIBUTION OF THIS DOCUMENT IS UNLIMITED

TECHNOLOGY DEVELOPMENT FOR HIGH POWER INDUCTION ACCELERATORS*

D. L. Birx and L. L. Reginato

Lawrence Livermore National Laboratory
University of California
Livermore, CA 94550

June 11, 1985

ABSTRACT

The marriage of Induction Linac technology with Nonlinear Magnetic Modulators has produced some unique capabilities. It appears possible to produce electron beams with average currents measured in amperes, at gradients exceeding 1 MeV/meter, and with power efficiencies approaching 50%. A 2 MeV, 5 kA electron accelerator has been constructed at the Lawrence Livermore National Laboratory (LLNL) to demonstrate these concepts and to provide a test facility for high brightness sources. The pulse drive for the accelerator is based on state-of-the-art magnetic pulse compressors with very high peak power capability, repetition rates exceeding a kilohertz and excellent reliability.

*Work performed jointly under the auspices of the U. S. Department of Energy by Lawrence Livermore National Laboratory under contract W-7405-ENG-48 and for the Department of Defense under Defense Advanced Research Projects Agency ARPA Order No. 4395 Amendment No. 31, monitored by Naval Surface Weapons Center under document number N60921-85-POW0001; and SDIO/BMD-ATC MIPR No. W3-RPD-53-A127.

MASTER
DISTRIBUTION OF THIS DOCUMENT IS UNLIMITED

EBB

I. INTRODUCTION

We are anticipating future needs beyond the capabilities of the spark-gap switches we developed for the Advanced Test Accelerator (ATA). We are continuing our efforts on magnetic pulse compressors that use nonlinear magnetic components and have designed reliable, high-current pulse compressors capable of generating continuous, 50 ns, 250 kV pulses at repetition rates exceeding 1 kHz.

The Laboratory's Advanced Test Accelerator (ATA), funded by the Defense Advanced Research Projects Agency, is a 50 MeV, 10 kA induction linear accelerator with a pulse length lasting up to 50 ns. Operation is normally at one Hertz average, however, the accelerator pulse power has the capability of burst mode operation at one kilohertz. This ten-pulse burst can be repeated every two seconds, giving the machine an average repetition rate of five pulses per second.

This performance, which makes the ATA unique among pulse power machines, came as the result of research on a novel, coaxial, gas-blown spark gap. The ATA contains modular, 250 kV induction- accelerator cells, each driven by a single pulse power unit. Each unit consists of a resonant transformer (1:10 step-up), a water-filled Blumlein pulse-forming line (PFL) for energy storage, and the aforementioned spark gap to discharge the PFL into the accelerator cell.

The initial commutation in the chain is performed by six fast recovery, glass-envelope thyratrons, four operating in the forward and two in the reverse direction. These tubular thyratrons, specially made for high-peak-power, low-duty-factor applications, transfer energy held in intermediate

storage through the 1:10 transformer and into the PFL. The transfer is completed in 20 μ s, and the tubes recover their ability to hold voltage in another 20 μ s.

A hiatus of 1 ms or more between pulses is necessary so the discharge products can be blown out of the spark gap. In theory, higher repetition rates could have been achieved by increasing the velocity of the gas that blows them out. Any significant increase is impractical, however, since the power required from the blower scales as the cube of the repetition rate, and it is already at 11.2 kW per gap for 1 kHz operation.

Figure 1, which schematically compares the pulse power requirements for the ATA and the Stanford Linear Accelerator (SLAC), suggests part of the reason why we needed to use spark gaps in the ATA. Although the pulse energy supplied to a SLAC radio-frequency accelerator section is essentially the same as that supplied to an ATA induction cell, the power level to the ATA is about a hundred times larger because the pulse is so much shorter.

The energy compression supplied by the spark gap (switch S_2 in Fig. 1b) supplied this power gain. The combination of a 250 kV operating voltage and a requirement for a current rise of 10 kA/ns (or 10^{13} A/s) forced us to use the crude but effective high-pressure spark-gap technology. However, such technology is not adequate to achieve high repetition rates for future applications.

Research into alternative switching schemes began almost before the first spark gaps went into use.

II. MAGNETIC PULSE COMPRESSION

The basic circuit for magnetic pulse compression is essentially the same as originally conceived in the 1950s. The fundamental principle involved is to use the large changes in permeability exhibited by saturating ferri-(ferro-) magnetic materials to produce large changes in impedance. Figure 2a shows the permeability changes in a representative saturable magnetic material, and Fig. 2b illustrates the standard technique for capitalizing on this behavior. First, a repetitive power source (using existing technology) generates the initial pulse. As this pulse propagates through the network, it goes through several states of compression until it achieves the desired output shape.

By using multiple stages as shown, it is possible to achieve a much larger effective change in impedance than can be obtained from a single stage. In fact, the effective change in impedance is limited only by the physical layout and materials properties. Figure 2c illustrates the results of the compression process.

The operation of this circuit can be described as follows. Capacitor C_1 charges through inductance L_0 until inductance L_1 saturates, becoming much less than L_0 . Once this happens, C_2 will begin to charge from C_1 through L_{1sat} , but since L_{1sat} is much less than L_0 , C_2 charges more rapidly than C_1 did. This process continues through the successive stages until C_n discharges into the load through $L_{n sat}$.

To make this process efficient, we design each of these successive stages so that saturation occurs at the peak of the voltage waveform. Segment 1 to 2

in the hysteresis loop of Fig. 2a is the active or high-permeability region during which the inductor impedes current flow; the leveling off of the curve at point 2, reached at the peak of the voltage waveform, indicates core saturation when the inductor achieves a low impedance. During segment 2 to 4, the core is reset to its original state, ready for the next cycle.

Aside from creating the ability to operate at increased repetition rates, the installation of magnetic pulse compressors appeared warranted on the basis of reliability and low maintenance. The benefits to the experimental program were also considerable.

III. THE ATA UPGRADE PROTOTYPE

Since October 1980, when we first began to work with magnetic switches, we have completed installation and final testing of a prototype magnetic switch package to replace the spark gaps in the ATA power units. The challenge was not to prove that a magnetic switch would do the job but rather to produce a unit that would fit the existing space, use as much of the existing equipment as possible, and be as inexpensive and reliable as possible.

The problem was further complicated by a desire for a peak repetition rate exceeding several kilohertz and an average repetition rate of a least 100 Hz. We also wanted the ability to operate at 1 kHz for up to one minute in every ten.

Figure 3 compares the two systems for driving ATA cells, the original one (containing a resonant transformer, a gas-blown spark gap, and a Blumlein line) and the new pulse compressor based on nonlinear magnetic elements. The latter is relatively inexpensive, and its performance surpasses that of any other system. Table I partially documents the capabilities demonstrated by this prototype.

Figure 4 compares the physical dimensions of the two systems. The existing pulse power unit is somewhat shorter than the new magnetic replacement, but it drives only one cell instead of two. The new unit consists of an input step-up transformer, one stage of compression to charge the transmission line, a second stage of compression, and the output coupling transformer. The output transformer can be housed as part of the magnetic pulse generator or as part of the load for best impedance matching.

Adding coupling transformers at both the input and the output of the magnetic pulse compressor improves the system's versatility by permitting it to achieve the desired output pulse while allowing the compression stages and the input switching device to operate at their most efficient values of voltage and current.

At this point in the evolution of the pulse-shaping hardware, we can design the transformer turns and the interstage capacitors as integral parts of the system. The resulting magnetic compressor is simple and extremely reliable, and it satisfies all the required performance specifications.

A desire to double the individual accelerator-cell voltage, coupled with the difficulty of sending 500 kV pulses around the system, prompted us to

adopt an alternate procedure. We send the output from the magnetic driver (about 170 kV peak) down to the accelerator cells via two 4Ω , semi-rigid, water-filled transmission lines. There, a pulse transformer provides a 3:1 voltage step-up and a ferrite pulse sharpener steepens the rise time. Figure 5 shows the physical layout and the two voltage waveforms.

A cross-sectional view of the accelerator cell connection is provided by Fig. 6. Here the ferrite shock line sharpeners and the CuSO_4 compensation loads can also be seen.

IV. THE HIGH BRIGHTNESS TEST STAND (HBTS)

The desire to construct a test stand for electron gun design provided an excellent opportunity to deploy this technology. While magnetic modulators had been deployed experimentally in isolated parts of both the Experimental Test Accelerator (ETA) and the Advanced Test Accelerator (ATA), this was the first case where they were solely responsible for the accelerator drive. A simplified schematic of the HBTS is provided by Fig. 7.

The two MAG I's each supply the 500 kV accelerating potential to two of the four accelerator cells. While the total accelerator potential has been run as high as 2 MeV, most of the experimental work to date has been performed between 1 and 1.5 MeV.

The primary goals of the HBTS are to generate a 1-2 kA electron beam of the highest brightness ($>10^5$ Amps/cm²-steradian) possible and at considerable average power. Upon meeting these requirements the HBTS will probably serve as the electron source for the ATA Free Electron Laser

experiments. A cross sectional view of the accelerator design showing the preliminary electron optics as well as the collimator diagnostic package; and some of the initial results provided are shown in Fig. 8. The electron beam quality measured at this time corresponded to a brightness of $2 \cdot 10^5$ Amps/cm² steradian.

The accelerator as shown in Fig. 8 is configured as a pentode electron gun employing a graphite field emission cathode.

While the experiments with this configuration were initially quite successful, none of various field emission cathodes tried were capable of meeting the high average power requirements. During operation above 50 Hz cw the cathodes soon showed signs of non-uniform emission and after several minutes ceased to emit at all. Upon returning to lower repetition rates the cathodes would recover to their original performance.

It is the belief of the authors that the operation of field emission cathodes is strongly dependent on the presence of condensed gas at the surface. Application of a high electric field stress is accompanied by the evaporation and subsequent ionization of this material thereby creating a plasma from whose sheath electrons can be extracted. Operation at high duty factors appears to deplete this gas supply.

Experiments are currently in progress which employ thermal cathode designs. It is hoped that the use of a dispenser cathode will allow us to meet both the brightness and average beam power requirement.

V. SUMMARY

In summary it seems that the marriage of Induction Accelerators with Magnetic Compression Technology has provided some unique capabilities.

As a final note it may be worth mentioning that while most of the accelerator operating time has been dedicated to research topics related to national defense, some initial experiments on radiation food processing have already been carried out in conjunction with the University of California at Davis, directed at documenting similarities and differences between this technique of radiation processing and the more conventional method of exposure to radioactive isotopes.

DISCLAIMER

This report was prepared as an account of work sponsored by an agency of the United States Government. Neither the United States Government nor any agency thereof, nor any of their employees, makes any warranty, express or implied, or assumes any legal liability or responsibility for the accuracy, completeness, or usefulness of any information, apparatus, product, or process disclosed, or represents that its use would not infringe privately owned rights. Reference herein to any specific commercial product, process, or service by trade name, trademark, manufacturer, or otherwise does not necessarily constitute or imply its endorsement, recommendation, or favoring by the United States Government or any agency thereof. The views and opinions of authors expressed herein do not necessarily state or reflect those of the United States Government or any agency thereof.

Table I

Comparison of output pulse parameters of the current spark-gap driver of the Advanced Test Accelerator and the MAG-1 prototype of an upgraded magnetic compression system.

Parameter	Spark Gap	Magnetic Compression
Peak output power, GW	2.5	10
Pulse rise time (10-90%) per cell, ns	18	15
Pulse length (FWHM), ns	70	80
Pulse energy, J	350	800
Efficiency (including resonant transformer), %	70	80
Voltage (2-cell driver) at 18 kA/cell, kV	100	300
Voltage (1-cell driver) at 25 kA/cell, kV	200	450
Pulse-to-pulse jitter at up to 1 kHz, ns	± 1	± 0.5
Peak burst rate (5 pulses), kHz	1	>10
Peak average repetition rate at 10% duty factor, kHz	0.1	1

- Fig. 1 Power conditioning comparison for RF linac and induction accelerator.
- Fig. 2 Diagrams outlining the operation of magnetic pulse compression.
(a) The hysteresis (B-H) loop of a typical saturable magnetic material. (b) Simplified schematic of a magnetic pulse compressor. The elements marked L_1 , L_2 , and L_n are nonlinear inductors. (c) Typical voltage waveforms associated with a magnetic pulse compressor.
- Fig. 3 Simplified schematics of pulse power chains for the ATA induction linear accelerator. (a) The present system, which uses a spark gap and Blumlein pulse formers. (b) The non-linear magnetic drive proposed for an upgrade of the ATA.
- Fig. 4 Geometric comparison between (a) the existing pulse power unit and (b) the prototype of the recently developed upgrade. The magnetic pulse compressor is longer and has about the same diameter as the existing pulse power unit, but it feeds two accelerator cells instead of one, making it possible to use only half as many units.
- Fig. 5 Initial tests of the MAG-1 (ATA upgrade prototype) driving a typical ATA cell. The diagram indicates the points in the circuit at which the voltages were measured.
- Fig. 6 HV transition to accelerator cell.
- Fig. 7 Initial configuration high brightness test stand (HBTS).
- Fig. 8 Cross-sectional view of the HBTS accelerator module; HBTS accelerator output waveforms, all pulses 20 ns/div.

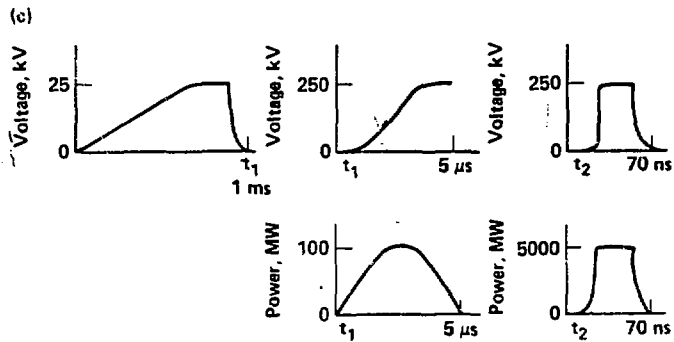
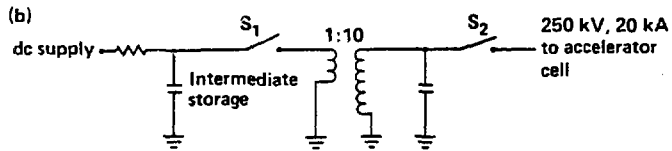
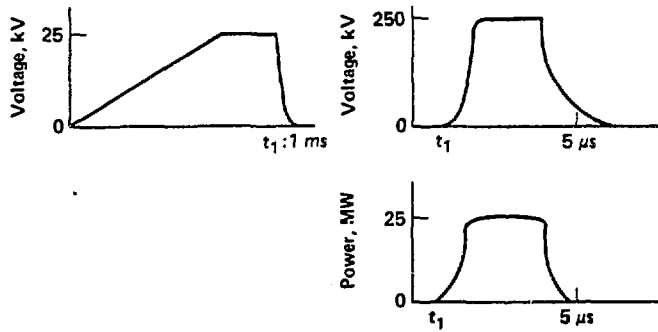
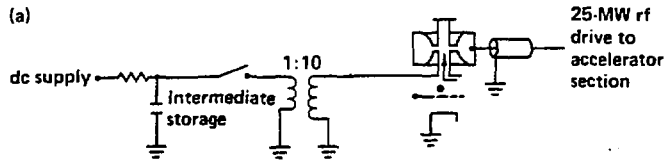


Figure 1

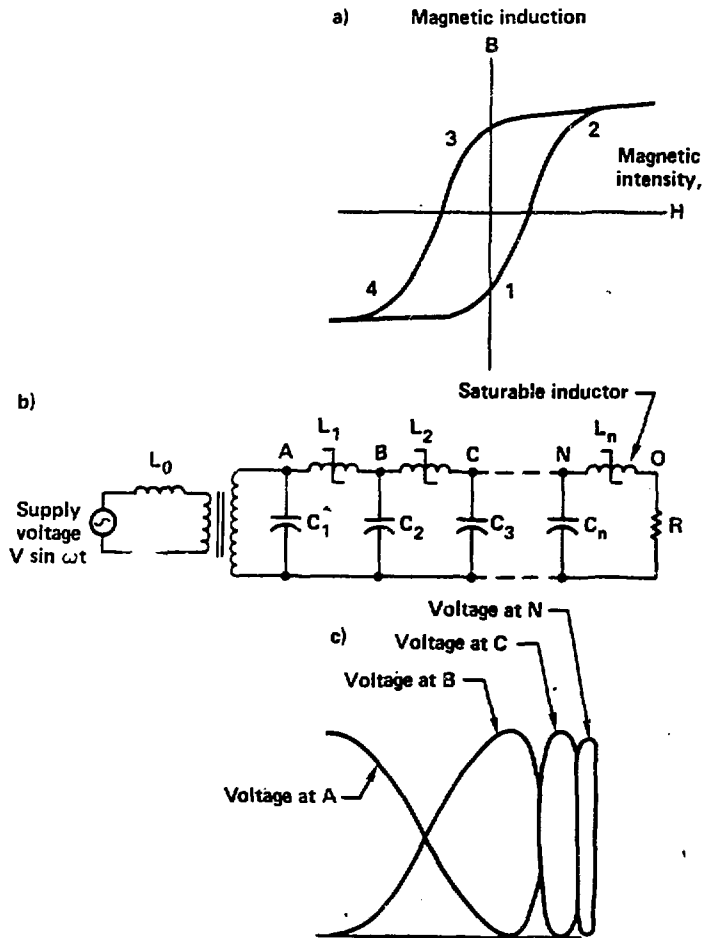


Figure 2

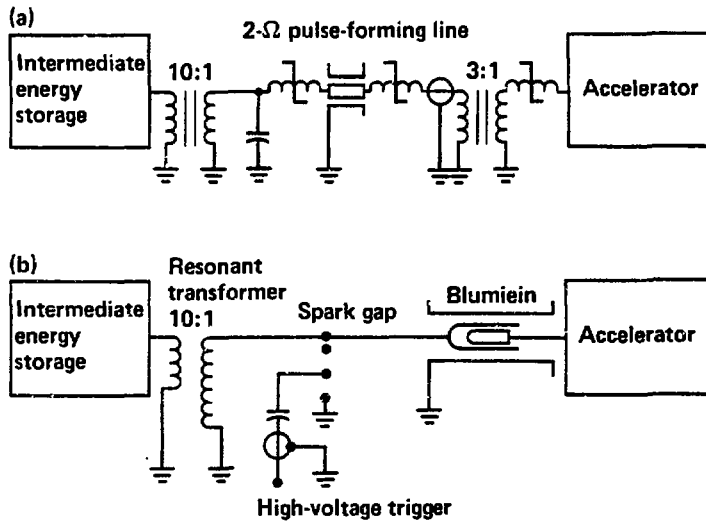


Figure 3

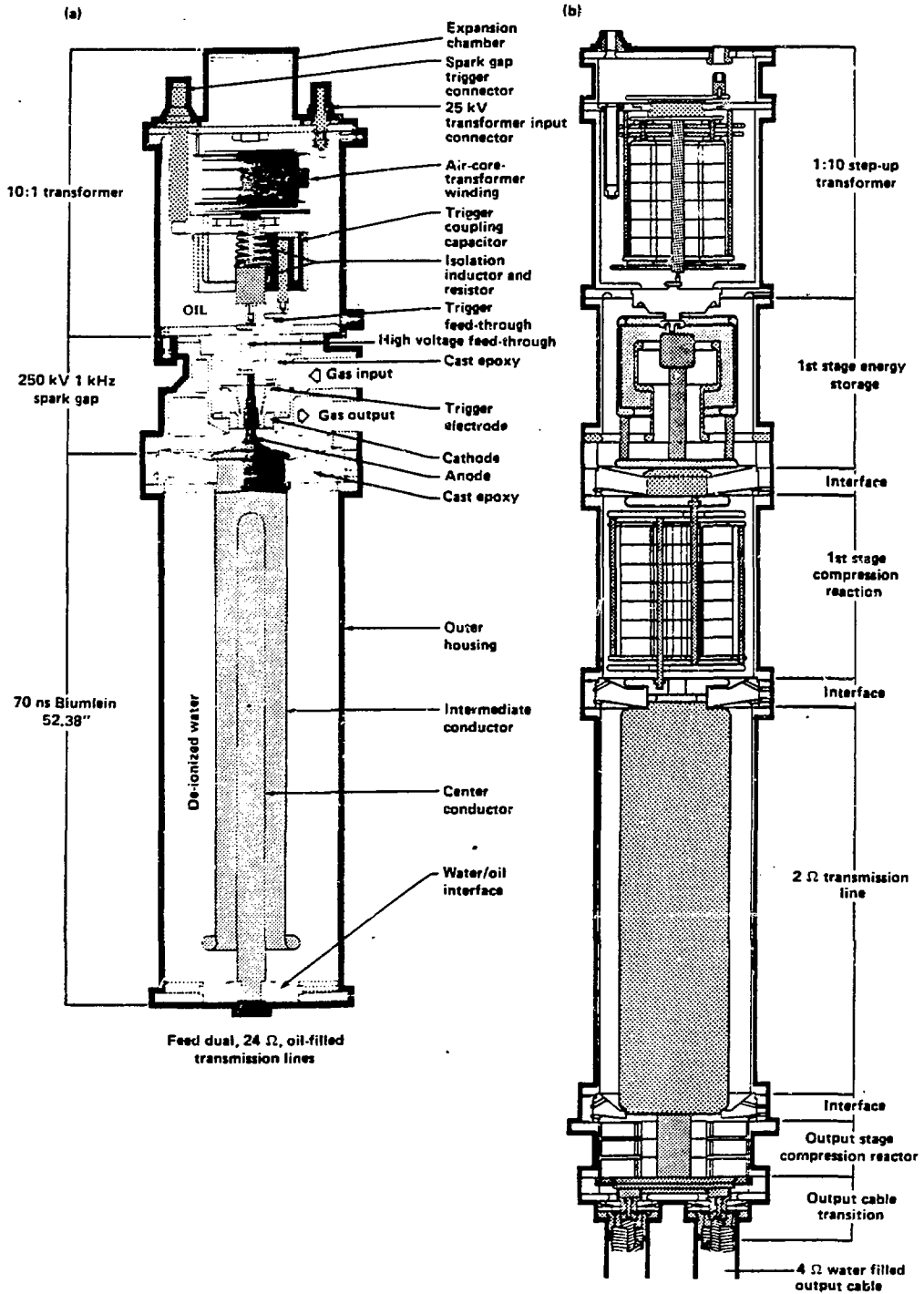


Figure 4

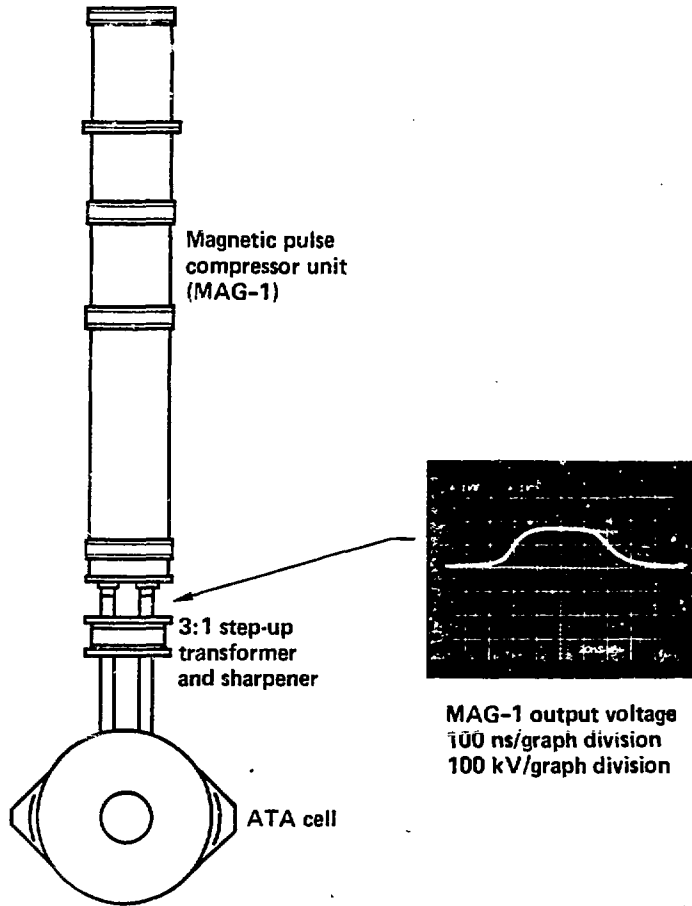


Figure 5

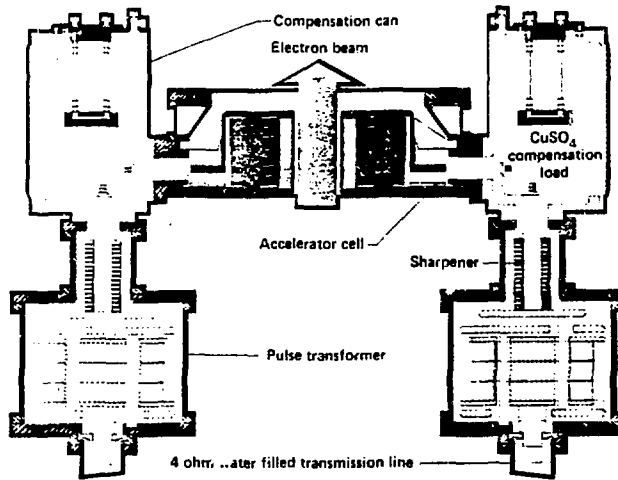


Figure 6

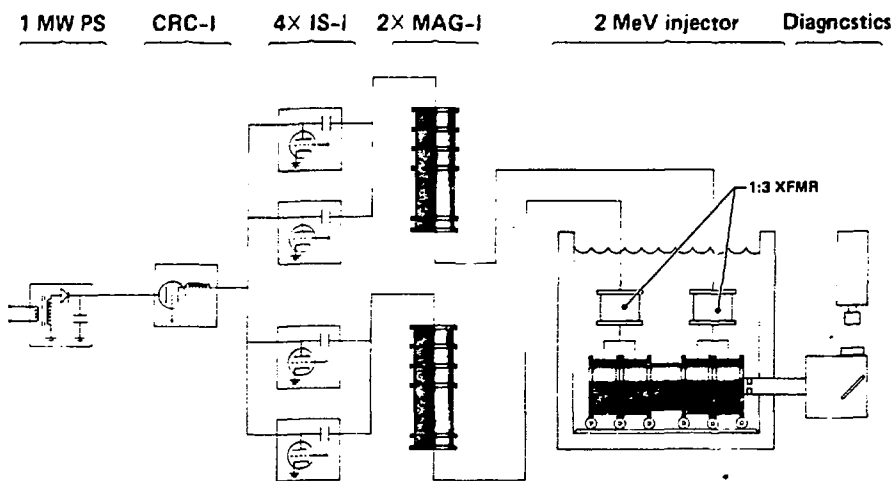


Figure 7

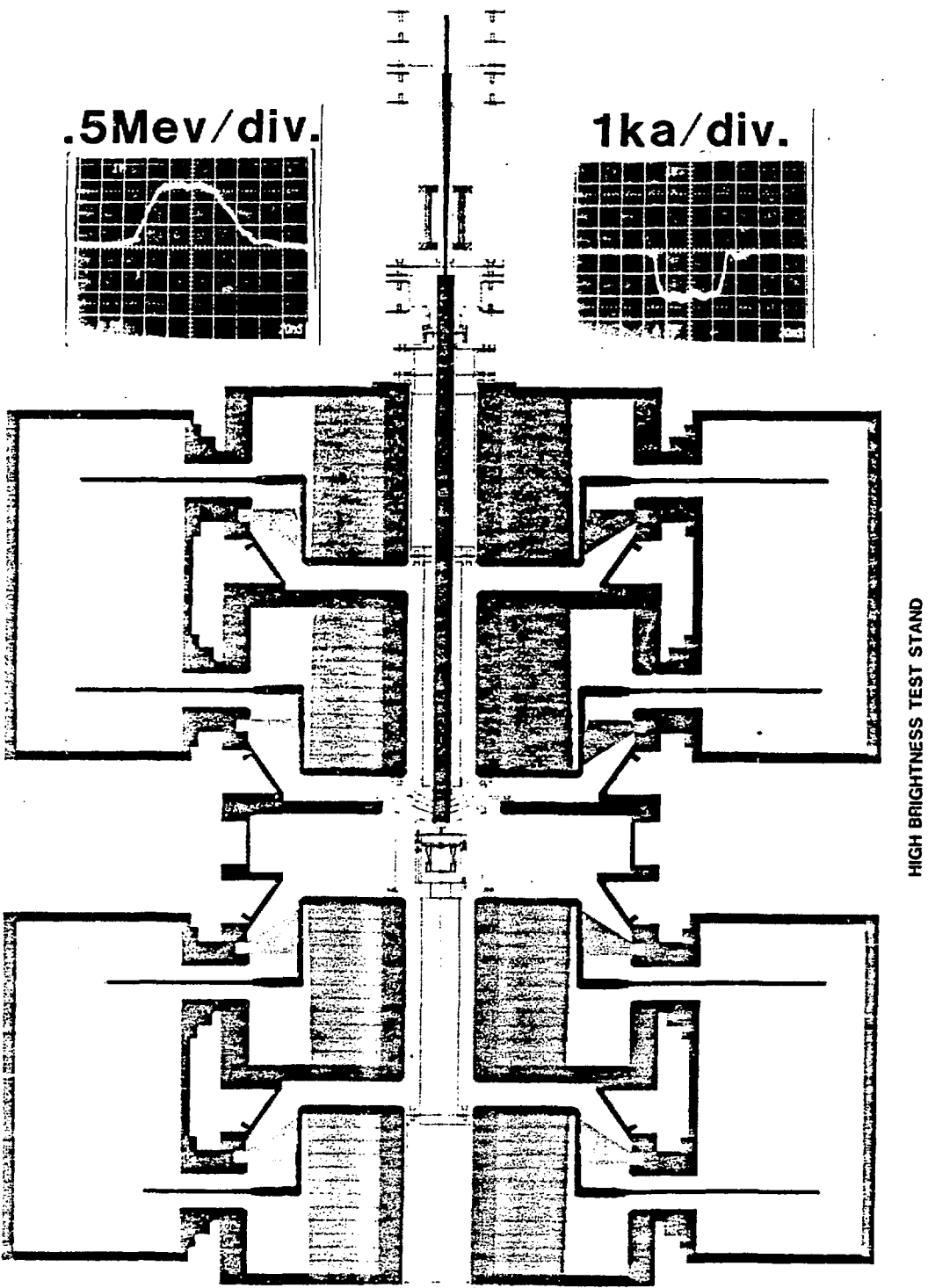


Figure 8